Observational and Modeling Studies of Impacts of the South China Sea Monsoon on the Monsoon Rainfall in the Middle-Lower Reaches of the Yangtze River During Summer

JIN Lijun[1] (靳丽君) and ZHAO Ping[1,2]* (赵 平)

1 *State Key Laboratory of Severe Weather, Chinese Academy of Meteorological Sciences, Beijing* 100081

2 *National Meteorological Information Centre, Beijing* 100081

(Received February 1, 2012; in final form February 1, 2012)

ABSTRACT

Based on the ERA-40 and NCEP/NCAR reanalysis data, the NOAA Climate Prediction Center's merged analysis of precipitation (CMAP), and the fifth-generation PSU/NCAR Mesoscale Model version 3 (MM5v3), we defined a monsoon intensity index over the East Asian tropical region and analyzed the impacts of summer (June–July) South China Sea (SCS) monsoon anomaly on monsoon precipitation over the middle-lower reaches of the Yangtze River (MLRYR) using both observational data analysis and numerical simulation methods. The results from the data analysis show that the interannual variations of the tropical monsoon over the SCS are negatively correlated with the southwesterly winds and precipitation over the MLRYR during June–July. Corresponding to stronger (weaker) tropical monsoon and precipitation, the southwesterly winds are weaker (stronger) over the MLRYR, with less (more) local precipitation. The simulation results further exhibit that when changing the SCS monsoon intensity, there are significant variations of monsoon and precipitation over the MLRYR. The simulated anomalies generally consist with the observations, which verifies the impact of the tropical monsoon on the monsoon precipitation over the MLRYR. This impact might be supported by certain physical processes. Moreover, when the tropical summer monsoon is stronger, the tropical anomalous westerly winds and positive precipitation anomalies usually maintain in the tropics and do not move northward into the MLRYR, hence the transport of water vapor toward southern China is weakened and the southwest flow and precipitation over southern China are also attenuated. On the other hand, the strengthened tropical monsoon may result in the weakening and southward shift of the western Pacific subtropical high through self-adjustment of the atmospheric circulation, leading to the weakening of the monsoon flows and precipitation over the MLRYR.

Key words: the South China Sea monsoon, precipitation in the middle-lower reaches of the Yangtze River, observational analysis, numerical simulation, interannual variability

Citation: Jin Lijun and Zhao Ping, 2012: Observational data and modeling studies of impacts of the South China Sea monsoon on the monsoon rainfall in the middle-lower reaches of the Yangtze River during summer. *Acta Meteor. Sinica*, **26**(2), 176–188, doi: 10.1007/s13351-012-0204-2.

1. Introduction

The East Asian monsoon includes the tropical monsoon over the South China Sea (SCS) and the western Pacific and the subtropical monsoon over the mainland of China, the Korean Peninsula, and Japan (He and Yu, 1986; Chen et al., 1991; Ding, 2004), in which the variability of summer monsoon over the Yangtze River (YR) area directly affects precipitation anomalies over eastern China, often resulting in large-scale flood disasters. There are close links between the East Asian tropical and subtropical monsoon rain belts. Particularly, there is a "+−+" correlation pattern in the interannual and interdecadal variations of precipitation among the SCS, YR reaches, and North China (Zhao and Zhou, 2009; Ding et al., 2007; Wang et al., 2008; Zhao et al., 2010). The variability of the tropical monsoon is associated with the subtropical monsoon precipitation through the East Asian-Pacific meridional teleconnection or the Pacific-Japan

Supported by the National Natural Science Foundation of China (40921003) and National Basic Research and Development (973) Program of China (2009CB421404).

*Corresponding author: zhaop@cma.gov.cn.

(Chinese version to be published)

(PJ) wave train (Nitta, 1987; Huang and Li, 1988).

Previous studies paid attention to not only the characteristics and mechanisms of the East Asian tropical monsoon establishment (Ding et al., 1994; Ding and Liu, 2006) but also the influence of the tropical monsoon climate on the East Asian subtropical monsoon (Chen et al., 1991; Zhang and Tao, 1998; Ding et al., 2004). The influences of oceanic conditions in the SCS and the warm pool of the western Pacific are specially emphasized (Huang and Sun, 1994; Liu et al., 2004; Huang et al., 2005; Zhao et al., 2010). These studies pointed out that the thermal conditions over the warm pool of the tropical western Pacific, particularly the convective activities near the Philippines, exert great effects on the onset of the East Asian subtropical monsoon and the advance and retreat of the monsoon rain belt. When the tropical western Pacific is warm (cold) during summer, the convective activities near the Philippines are strong (weak), the time of the SCS summer monsoon onset is early (late), the ridge of the subtropical high over the western North Pacific moves pronouncedly northward (stays in a northward position), and the precipitation decreases (increases) between the YR and Huaihe River reaches and increases (decreases) over North China.

Convections over the tropical western Pacific are also related to the seasonal advance and retreat of the ridge of the western North Pacific subtropical high and the East Asian upper-level jet streams and their variations in intensity. For example, Lu (2004) found that a climatic anomaly near the Philippines may affect the position of the rain belt over the subtropics of East Asia through changing the low-level subtropical high ridge over the western North Pacific and the upper-level atmospheric circulation over East Asia.

On the interannual and interdecadal timescales, the influences of ENSO in the tropical eastern Pacific and the SST in the Indian Ocean on the East Asian monsoon and rainfall are also noted (Zou and Ni, 1997; Wang et al., 2000; Zhang, 2001; Wang, 2002; Qian, 2009; Yao and Qian, 2011; Zhao et al., 2010). On the seasonal and intraseasonal scales, the tropical low-frequency oscillations exert important impacts on not only the tropical climate systems but also atmospheric circulation and climate over the entire Asian monsoon region (Li et al., 2001; Wen et al., 2006). The 30–60-day oscillation from the equator meets the southward-propagating 30–60-day oscillation near 25°–30°N that comes from the mid and high latitudes of East Asia, which may affect the intensity and position of precipitation over eastern China (Chen and Xie, 1988; He and Yang, 1992).

Although previous studies on the tropical climates over the SCS and the subtropical summer monsoon over eastern China have made great progress, there are still some scientific questions that need to be investigated in depth in this field. For example, some new results from observations and numerical simulations showed that on the seasonal scale, the southwest monsoon and associated rain belt over the YR basin do not result from a northward shift of the SCS monsoon rain belt but originate directly from a northward advance of spring southwesterly winds and the associated rain belt to the south of the YR, and the variation of thermal contrasts between the East Asian land and its adjacent oceans has a substantial effect on the northward advance of the spring rain belt (Chen et al., 2001; Zhao et al., 2007; He et al., 2007; Qi et al., 2007; Zhao et al., 2009a, b). Then, do these results suggest that the tropical monsoon has no influence on the YR monsoon rainfall anomalies? Could the tropical southwesterly winds and rainfall directly shift northwards to the YR and then cause an in-phase variation of the YR monsoon and rainfall on the interannual scale? To answer these questions, it is necessary to investigate the effects of anomalous tropical monsoon intensity over the SCS on the YR monsoon and rainfall through observational data analysis and numerical simulations.

Because zonal wind is dominant over the tropics of East Asia, it has been used extensively to examine the variability of the SCS tropical monsoon (Qian and Yang, 2000; Wang et al., 2004; Zhao et al., 2009b). In this study, we use the zonal wind over the SCS and the adjacent areas to indicate the East Asian tropical monsoon intensity. The influences of the summer tropical monsoon anomalies on southwest monsoon and rainfall over the middle-lower reaches of the YR (MLRYR) are investigated based on observational data and numerical simulations. The purpose of this study is to reveal the interannual relationships between the tropical monsoon over the SCS and the southwest monsoon over southern China.

2. Observational data analysis of relationships between the SCS monsoon and the MLRYR monsoon

In the observational data analysis, we utilize monthly mean ERA-40 reanalysis data of the European Centre for Medium-Range Weather Forecasts (ECMWF) during 1958–2001 (Uppala et al., 2005), the raingauge data from 160 surface weather stations of China, and the NOAA Climate Prediction Center's merged analysis of global pentad mean precipitation (CMAP) (Xie and Arkin, 1997). The significance of the correlation and composite analyses used in this study is assessed by the Student's *t*-test. All the results in this study are at the 95% significance level unless otherwise stated. Because the East Asian subtropical monsoon rainfall occurs mainly over the MLRYR during June–July, we will focus on the effects of tropical monsoon on monsoon rainfall over the MLRYR during this period.

Figure 1a shows the climatology of summer (June–July) 850-hPa winds. It is seen that the westerly wind exceeding 5 m s^{-1} prevails over a large area from the Arabian Sea to the SCS, indicating the prevalence of the Asian tropical summer monsoon. Because the zonal wind component is much larger than the meridional wind component, which is consistent with the previous studies (Webster and Yang, 1992; Webster et al., 1998; Qian and Yang, 2000; Wang et al., 2004; Zhao et al., 2007, 2009b), the 850-hPa zonal wind is used to indicate the variability of the Asian tropical monsoon intensity. On the standard deviation map of 850-hPa zonal wind (Fig. 1b), the standard deviation above 2 m s^{-1} covers a large tropical area from the Indo-China Peninsula to western Pacific via the SCS, with values greater than 5 m s^{-1} spreading between 120° and 130°E. By referring to the distributions of tropical westerly wind intensity and its standard deviation, the 850-hPa zonal wind averaged over the tropical region (5°–17.5°N, 100°–130°E) from the Indo-China Peninsula to western Pacific is used to indicate the variability of the SCS tropical monsoon intensity, called the SCS monsoon (SCSM) index. It is seen from the correlation map between the summer SCSM index and the simultaneous 850-hPa zonal wind (figure omitted) that the significant positive correlation exceeding 0.6 covers the tropics from India to western Pacific, with the maximum value exceeding 0.8 over the region from the Bay of Bengal to eastern Philippines, which indicates that the SCSM index defined in this study can well reflect the variation features of lower-tropospheric zonal wind over the SCS and adjacent areas.

Figure 2 shows the temporal variation curve of the summer SCSM index during 1958–2001. This index remarkably exhibits interannual variability. We separately select seven strongest and weakest SCSM-index years to perform a composite analysis, in which the seven strongest index years are 1965, 1972, 1982, 1985, 1990, 1994, and 1999, and the seven weakest index years are 1959, 1964, 1966, 1983, 1995, 1996, and

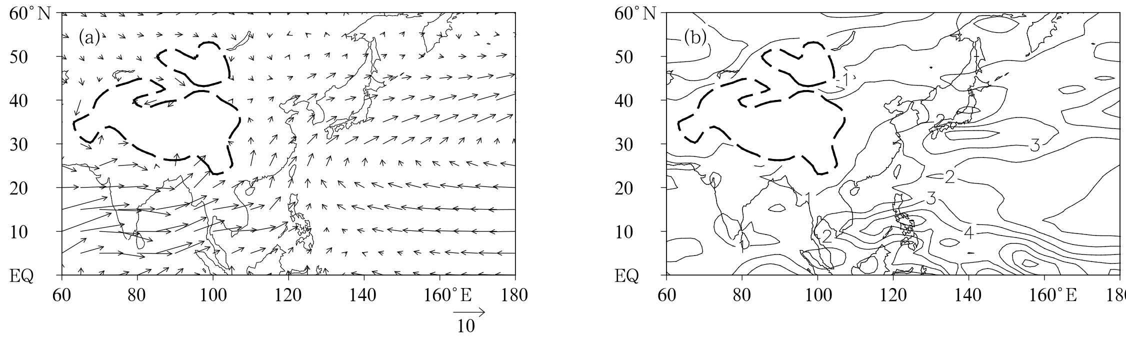

Fig. 1. (a) Climatology of June–July mean 850-hPa winds (m s^{-1}) and (b) standard deviation of 850-hPa zonal wind (m s^{-1}) for the period 1958–2001. The thick dashed lines indicate the topographic contour of 1500 m.

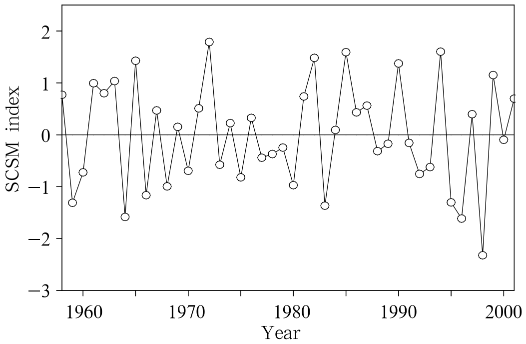

Fig. 2. The temporal curve of the June–July mean SCSM index during 1958–2001.

1998. Figure 3a shows the composite difference of 850-hPa winds between the strong and weak SCSM-index years. It is seen that significant westerly wind anomalies prevail over the tropics from Southeast Asia to western Pacific. This indicates a stronger westerly wind over these regions when the SCSM index is higher. The strengthened tropical westerly wind also enhances the local low-level air convergence (figure omitted), leading to anomalous upward motion (Fig. 3c) and increased rainfall over the tropical monsoon region. Figure 4a shows the correlation coefficient between the summer SCSM index and the simultaneous CMAP rainfall during 1979–2001. It is seen that significant positive correlations appear from the SCS to the tropical western Pacific, indicating a more tropical monsoon rainfall, when the tropical westerly wind is stronger. These results suggest that the summer SCSM index can indicate the variations of the tropical monsoon and rainfall over the SCS and the adjacent areas.

When the SCS tropical monsoon is stronger (weaker), however, the southwest monsoon does not synchronously strengthen (weaken) over the YR and Huaihe River reaches and the area to the south. In Fig. 3a, corresponding to a stronger tropical monsoon, a large-scale anomalous cyclonic circulation appears near 20°N over the SCS-western Pacific region. On the composite difference map of 850-hPa geopotential height (Fig. 3b), large-scale significant negative anomalies appear from southeast of the Tibetan Plateau to the tropical western Pacific, with their negative central value of −20 dgpm over the northern SCS. The northern boundary of the western Pacific subtropical high ridge with the contour 1460 dgpm along

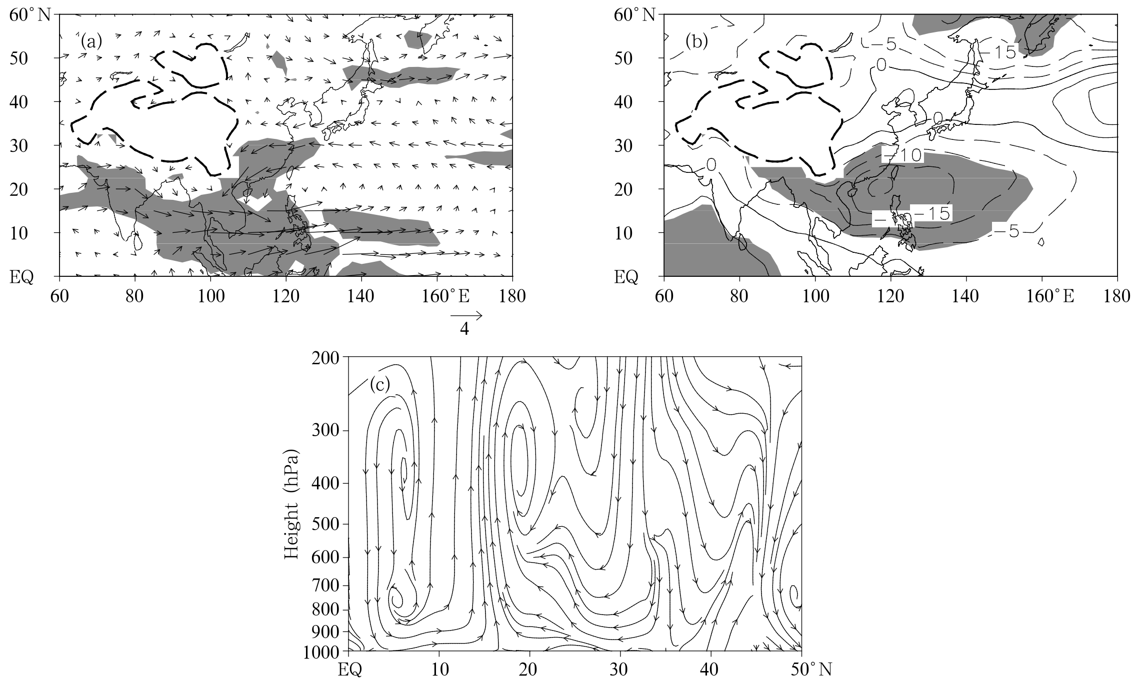

Fig. 3. (a) Composite difference of June–July 850-hPa winds (m s^{-1}), (b) 850-hPa geopotential height (dgpm), and (c) latitude-height cross-section of vertical circulation along 115°E between the strong and weak SCSM-index years. In (a) and (b), the shaded areas are at the 95% confidence level.

130°E is located near 25°N (figure omitted), more southward compared to 29°N in a weaker tropical monsoon. This anomalous feature in the atmospheric circulation indicates a southward and weak ridge over the subtropical western Pacific. At this time, the northeasterly wind anomalies to the north of the anomalous cyclonic circulation center prevail over the land of eastern China. On the climatological mean map, the southwesterly winds prevail over this region during summer. Thus, presence of the northeasterly wind anomalies indicates that the southwesterly flow weakens over southern China when the East Asian tropical monsoon is stronger. On the composite difference map of the meridional-vertical circulation (Fig. 3c), there is an anomalous circulation center in the troposphere near 20°N, with anomalous downward motion over the subtropics (27°–33°N) of East Asia that accompanies anomalous upward motion over the tropics. Meanwhile, the weakened low-level southwesterly flow does not favor the transport of water vapor toward the mainland of China (figure omitted). Therefore, corresponding to the weakened southwest monsoon and upward motion over the subtropics, there is less rainfall over the MLRYR. Accordingly, as shown in Fig. 4a, significant negative correlation coefficients appear between 26° and 32°N of eastern China. This link between the summer SCSM index and rainfall over eastern China is also observed on the composite difference map of summer rainfall from surface raingauge stations between the strong and weak SCSM-index years (Fig. 4b). In Fig. 4b, negative rainfall anomalies appear over the MLRYR.

The above analysis reveals that there is a close relationship of the SCS tropical monsoon and rainfall with those of the MLRYR on the interannual scale. This relationship shows an out-of-phase variation feature, that is, the southwest monsoon over the southern China often weakens when the tropical monsoon strengthens. This result is similar to that of the previous studies (Ding et al., 2007; Wang et al., 2008). Qian et al. (2009) showed a negative correlation between the June–August rainfall in the SCS-tropical western Pacific monsoon region and that of the YR basin on the interannual scale. Then, does this statistical relationship between the tropical monsoon and the monsoon in the MLRYR reflect an effect of the former on the latter? In the following section, we further analyze the impacts of changes in the tropical monsoon intensity on the monsoon and rainfall over the MLRYR through sensitivity experiments of a numerical model.

3. Numerical simulations on the impacts of the SCS monsoon on the MLRYR monsoon and rainfall

3.1 Model and experimental design

In order to conveniently investigate the effects of the SCS tropical monsoon on the YR monsoon and rainfall using a numerical model, we utilize the nonhydrostatic mesoscale model MM5v3 developed by the PSU/NCAR, in which a simple ice-phase precipitation

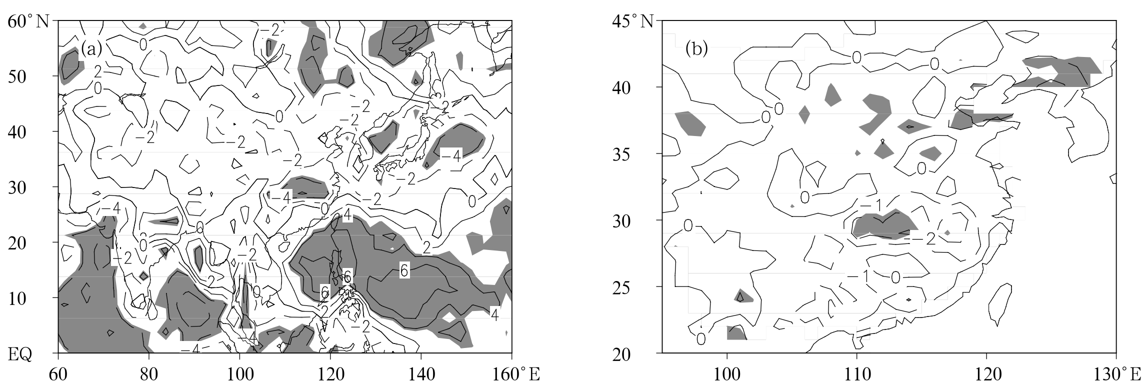

Fig. 4. (a) Correlation coefficient between the June–July SCSM index and the synchronous CMAP precipitation for the period 1979–2001, and (b) composite difference of June–July total precipitation (×100 mm) at surface weather stations between the strong and weak SCSM-index years. The shaded areas are at the 90% confidence level.

scheme, the Grell cumulus parameterization scheme, the MRF (Medium-Range Forecast) model planetary boundary layer scheme, and a cloud radiational scheme are selected. Moreover, a relaxation approximation scheme is used as the lateral boundary condition. In the present study, the model domain has a horizontal resolution of 80 km, with 72 and 50 grid points in the east-west and south-north directions, respectively. The model atmosphere in the vertical direction is separated into 23 layers, with the top of the model atmosphere at 100 hPa. Some studies have shown that the MM5v3 can be applied to simulating atmospheric circulation and precipitation over East Asia (Lau et al., 1998; Tang et al., 2004). Using this model, Zhao et al. (2009a) investigated the impacts of ocean-land thermal contrasts over the East Asian region on southwest monsoon and rainfall over southern China for 2004 and 2005.

In order to simulate impacts of the SCS tropical monsoon intensity anomalies on the YR monsoon rainfall through adjusting atmospheric conditions at the southern boundary of the model domain, the model domain is centered at 30°N, 110°E and its southern boundary is approximately set at 15°N. In the present study, experiments A, B, and C are designed to examine the impacts of the SCS tropical monsoon on the YR monsoon. Southwesterly winds over eastern China are strong in 2004 and weak in 2005 (Zhao et al., 2009a; Yao and Qian, 2011), thus we select these two years to perform comparative simulations.

Experiment A is a control experiment for assessing the capability of the MM5v3 model. Consistent with Zhao et al. (2009a), in experiment A, the atmospheric initial and lateral boundary data and land surface data come from the 4-time daily reanalysis dataset of the NCEP/NCAR with a horizontal resolution of $1°\times1°$ (Kalnay et al., 1996), and the sea surface temperature data come from the daily analysis dataset of the NCEP–Environmental Modeling Center with a horizontal resolution of $0.5°\times0.5°$ (Gemmill et al., 2007). The time step of the model integration is set at 240 s. The SCS tropical monsoon often breaks out in May (Lau and Yang, 1997; Webster et al., 1998). To understand how the tropical monsoon and rainfall anomalies propagate during May and July after the onset of the tropical monsoon, the MM5v3 model is run from 0000 UTC 1 May to 31 July, in which the atmospheric lateral conditions and the land surface conditions are refreshed with an interval of 6 h.

In experiment B (with strengthened SCS tropical monsoon), the atmospheric data at the southern boundary of the model domain corresponding to a stronger tropical westerly wind replace those in experiment A and remain unchanged during the entire integration period. Experiment B is described in detail as follows. Based on the 4-time daily NCEP/NCAR reanalysis data during May and July, we firstly select the time when there is a strong lower-tropospheric (below 700 hPa) westerly wind at the southern boundary of the model domain. Then, the geopotential height, temperature, zonal wind, meridional wind, and humidity from the reanalysis dataset along the southern boundary-vertical cross-section at this time are put into the model to replace atmospheric data at the southern boundary in experiment A throughout the model integration period, so that the tropical monsoon is always strong during May and July in experiment B relative to experiment A.

Experiment C is the same as experiment B but it selects a weak lower-tropospheric westerly wind at the southern boundary of the model domain. In order to increase the reliability of sensitivity experiments, we use the atmospheric data at the southern boundary corresponding to different strong (weak) tropical westerly winds to repeat experiment B (C) five times and the mean of five model outputs is used as the result of experiment B (C). It is seen from the following analysis that the simulation results are in good consistency with observations, which demonstrates that the configuration of experiments B and C is reasonable.

3.2 Simulation results

Figure 5a shows the time-latitude cross-section of 850-hPa meridional wind of the NCEP/NCAR reanalysis along 110°–120°E during the 25th and 42th pentad. It is seen that the southerly wind prevails to the south of 30°N most of the time, with the central value exceeding 8 m s^{-1}. In the June–July 850-hPa wind and geopotential height fields (Fig. 5b), large-scale southwesterly winds prevail over the mid-low latitudes of the Asian continent and the coastal areas and there is a low pressure system to the southeast of the Tibetan Plateau, with a ridge over the mid-low latitudes of the western Pacific. Figure 5c shows the time-latitude cross-section of the CMAP rainfall along 110°–120°E. In this figure, the rain belt over southern China is mainly located to the south of 30°N during May and June and then remarkably moves northward, maintaining generally to the north of 30°N. These results exhibit that the atmospheric circulation and rainfall over eastern China in 2005 have a major feature of the subtropical monsoon (Chen et al., 1991; Ding, 2004). Compared with Fig. 5, it is seen in Fig. 6 that experiment A captures major features of the temporal evolution (Fig. 6a) and horizontal distribution (Fig. 6b) of the southwesterly winds over East Asia during May and July 2005. The temporal evolution of the simulated rain belt over eastern China (Fig. 6c) shows that although the simulated rainfall is slightly northward in position and is larger in value compared with the observation, the temporal evolution of the simulated rain belt and its northward shift during summer are consistent with those in Fig. 5c. These results indicate that the model is able to capture the major features of the May–July southwesterly wind and rainfall over the East Asian monsoon region in 2005 in experiment A. Thus, the MM5v3 model may be applied to studying impacts of the tropical monsoon intensity changes in experiments B and C.

Figure 7a shows the time-latitude cross section of the difference of the simulated 850-hPa zonal wind between experiments B and C along 110°–120°E in 2005. It is seen that significant westerly wind anomalies always maintain near the southern boundary of the model domain, which indicates that the westerly wind is stronger in experiment B than in experiment C during the entire integration period. On the difference map of the simulated June–July 850-hPa wind between experiments B and C (Fig. 7b), significant southwesterly wind anomalies prevail over the tropics from the Indo-China Peninsula to the western Pacific, indicating a stronger tropical southwesterly flow in

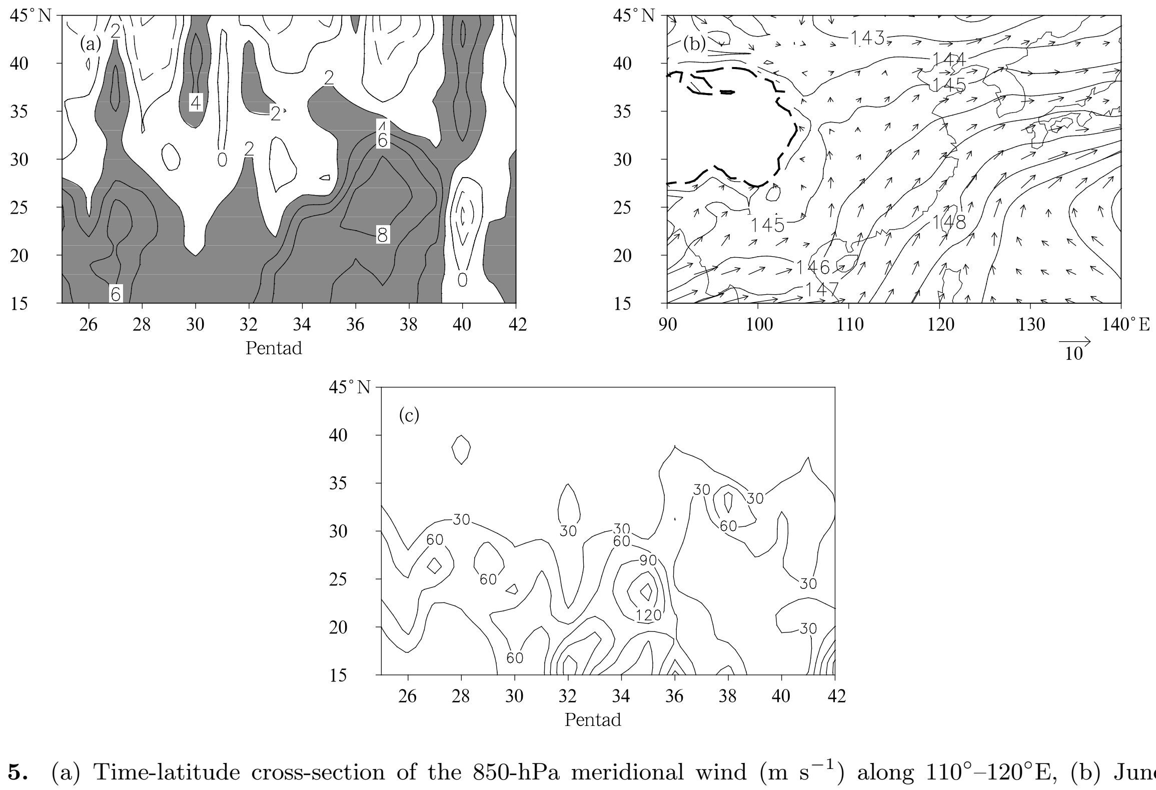

Fig. 5. (a) Time-latitude cross-section of the 850-hPa meridional wind (m s^{-1}) along 110°–120°E, (b) June–July 850-hPa winds (vector; m s^{-1}) and geopotential height (contour line; ×10 dgpm) in the NCEP/NCAR reanalysis, and (c) time-latitude cross-section of the CMAP precipitation (mm pentad^{-1}) in 2005.

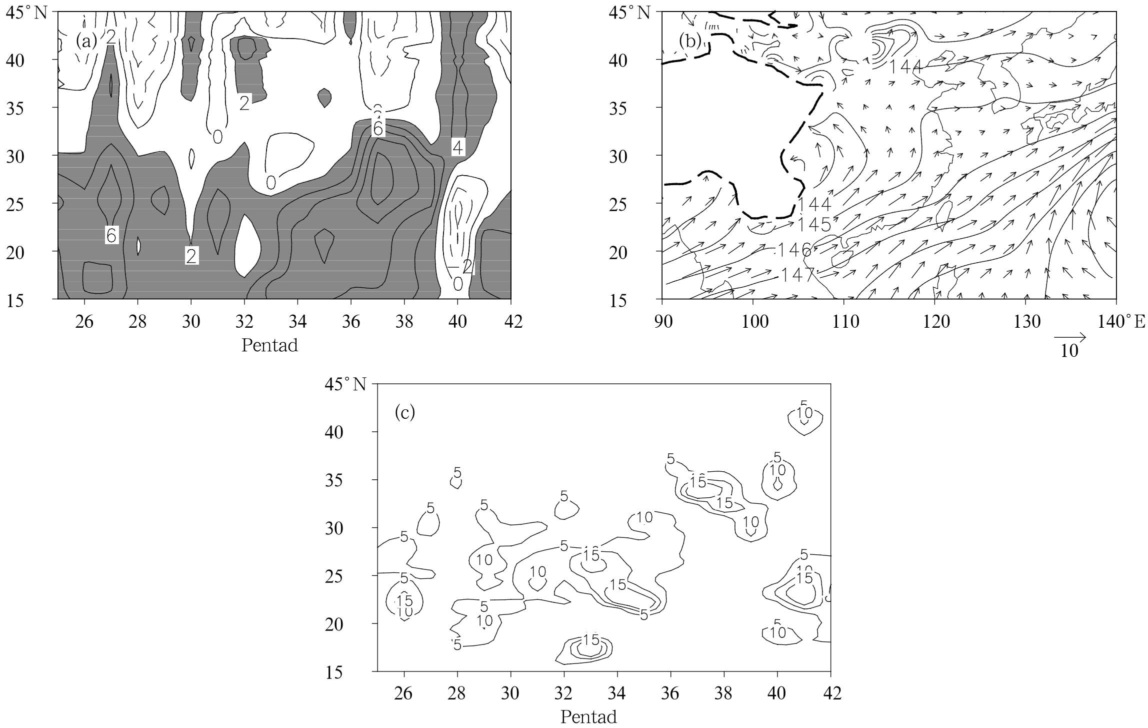

Fig. 6. (a) Time-latitude cross-section of the simulated 850-hPa meridional wind (m s^{-1}) along 110°–120°E, (b) June–July 850-hPa winds (vector; m s^{-1}) and geopotential height (contour line; ×10 dgpm), and (c) time-latitude cross-section of rainfall (×10 mm pentad^{-1}) along 110°–120°E in experiment A in 2005.

experiment B than that in experiment C. Corresponding to these variations of the tropical atmospheric circulation between experiments B and C, significant monsoon rainfall anomalies appear over the SCS and the adjacent tropical areas. In Fig. 8a, significant positive rainfall anomalies occur to the south of 20°N during the entire integration period. On the horizontal map (Fig. 8b), significant positive rainfall anomalies cover the oceans to the southeast of the mainland of China, indicating more monsoon rainfall over the tropical SCS, corresponding to a stronger tropical southwesterly flow and strengthened tropical monsoon rainfall. It is evident that the enhanced and weakened SCS tropical monsoons are simulated in experiments B and C, respectively. Meanwhile, it is noted that the simulated tropical westerly wind and positive rainfall anomalies mainly stay over the tropics, not showing a striking northward shift to the subtropical mainland of eastern China.

Over the subtropics of East Asia, a large-scale anomalous cyclonic circulation appears over East Asia, Southeast Asia, and the mid and low latitudes of the western Pacific, with its anomalous circulation center near 20°N over the western Pacific, and northeasterly wind anomalies to the north of the anomalous cyclonic center prevail over eastern China (Fig. 7b). The easterly wind anomalies always maintain over southern China during the entire model integration period (Fig. 7a). Corresponding to this anomalous cyclonic circulation, there are significant negative anomalies of 850-hPa geopotential height over East Asia and the western Pacific, with a geopotential height difference of –55 dgpm over the Pacific near 20°N (Fig. 7c). It is found that when the East Asian tropical monsoon strengthens, the ridge of the subtropical high over the western Pacific is located at a southward position (figure omitted), and the southward and weak subtropical high ridge corresponds to a weak southwesterly flow over eastern China in summer. This features a weak monsoon over the YR reaches, not favoring the transport of water vapor toward the mainland of China. On the simulated difference map of meridional vertical circulation along 115°E (Fig. 7d), upward motion anomalies appear in the troposphere to the south of 23°N, with downward motion anomalies in the troposphere within 25°–37°N. Because these simulated anomalous characteristics are basically consistent with those in Fig. 3, the atmospheric circulation anomalies over southern China associated with the tropical monsoon shown in Fig. 3 can be forced by changing the East Asian tropical southwesterly wind intensity, which reflects the impact of the tropical monsoon on the YR monsoon. This impact of the tropical monsoon on the atmospheric circulation over southern China may be explained as follows.

Compared to experiment C, the strengthened southwesterly flow over the tropics in experiment B enhances the local low-level air horizontal convergence. In theory, smaller regional-scale cyclonic circulations may occur within the convergence region of a large-scale heterogeneous southwesterly wind through the horizontal advection function of large-scale flows (Zhao and Zhou, 2001). Meanwhile, based on the vorticity equation, the air convergence may also produce positive vorticity, forming a cyclonic circulation. Therefore, the cyclonic circulation anomalies shown in Fig. 7b may occur within the low-level strengthened tropical convergence region in experiment B, with the northeasterly wind anomalies to the north of the anomalous cyclonic center prevailing over southern China.

Corresponding to the variations of atmospheric circulation over East Asia, significant rainfall anomalies appear over the MLRYR. It is seen from Fig. 8a that significant negative rainfall anomalies generally appear between 23° and 30°N during late spring and early summer and move northwards to 30°–38°N during mid summer. On the horizontal map (Fig. 8b), significant negative rainfall anomalies are located from the YR–Huaihe River reaches to the subtropical western Pacific, with the anomaly center to the south of the YR. These results indicate that when the SCS tropical monsoon strengthens, the YR monsoon rainfall generally shows a weakened feature. These simulated

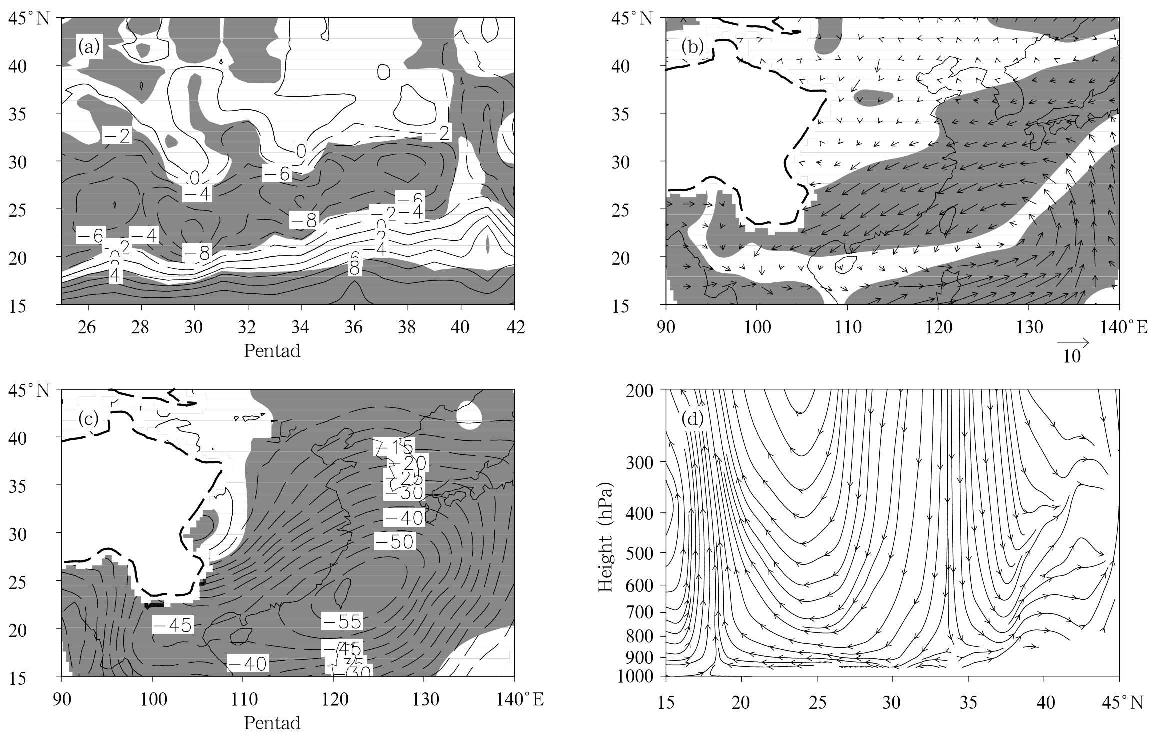

Fig. 7. (a) Time-latitude cross-section of composite difference (experiment B minus experiment C) of the simulated 850-hPa zonal wind (m s^{-1}) along 110°–120°E in 2005, in which the shaded areas are at the 95% confidence level, (b) as in (a), but for June–July mean 850-hPa winds (m s^{-1}), (c) as in (a), but for 850-hPa geopotential height (dgpm), and (d) as in (a), but for latitude-height cross-section of vertical circulation along 115°E.

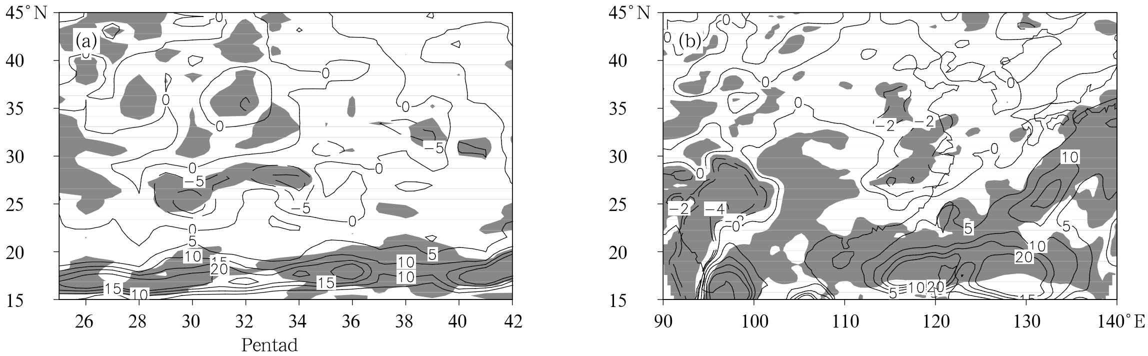

Fig. 8. (a) As in Fig. 7a, but for precipitation (×10 mm pentad^{-1}), and (b) as in Fig. 7b, but for June–July total precipitation (×100 mm).

rainfall variation features over the YR reaches are basically consistent with those of the observation shown in Fig. 4.

In order to verity the conclusions obtained from the simulations in 2005, we analyze the simulated results in 2004 when there was a weaker southwest monsoon over eastern China. Compared to the observations, it is seen that the MM5v3 model in experiment A also captures basic characteristics of monsoon circulation and rainfall over East Asia (figure omitted). Then, we analyze the simulated differences between experiments B and C. Figure 9a shows the time-latitude cross-section of the simulated 850-hPa zonal wind difference between experiments B and C along 110°–120°E in 2004. In this figure, positive zonal wind anomalies maintain over the tropics near 15°N during the integration period, indicating a stronger westerly wind simulated in experiment B relative to experiment C, that is, the model in experiment B simulates a strong tropical monsoon. The simulated westerly wind anomalies mainly stay over the tropics, not moving northward to the subtropical land, and the easterly wind anomalies largely prevail over southern China. On the horizontal map of the June–July wind

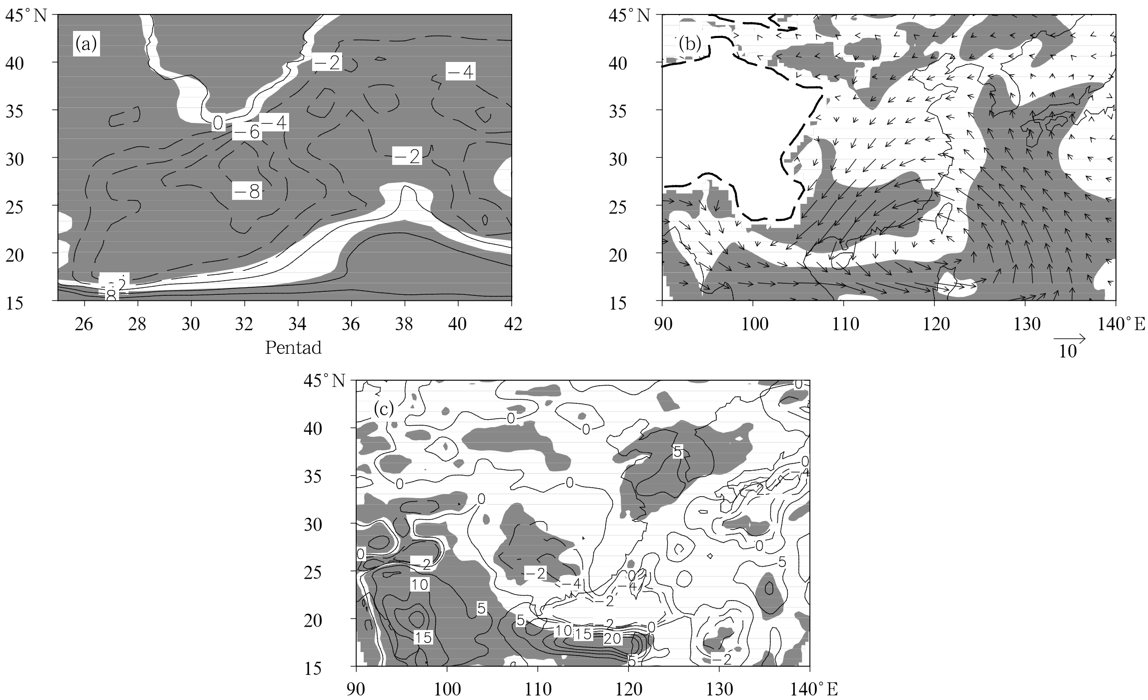

Fig. 9. (a) As in Fig. 7a, but for 2004, (b) as in Fig. 7b, but for 2004, and (c) as in Fig. 8b, but for 2004.

difference (Fig. 9b), a significant anomalous cyclonic circulation occurs over East Asia and its coasts, with the circulation center near 20°N, 120°E. The westerly wind anomalies appear over the tropics, while the northeasterly wind anomalies prevail over eastern China. Corresponding to these anomalies in the atmospheric circulation, significant positive rainfall anomalies appear over the tropics from the Indo-China Peninsula to the SCS during June and July, while negative rainfall anomalies appear over eastern China between 20° and 35°N (Fig. 9c). Evidently, for 2004, when the SCS tropical monsoon strengthens, the local monsoon rainfall increases, while the southwesterly wind over southern China and the associated rainfall weaken. Thus, the anomalous characteristics of the simulated atmospheric circulation and rainfall in 2004 are generally consistent with those in 2005, which supports the conclusions obtained from the simulation in 2005.

4. Conclusions and discussion

In this study, using the ERA-40 and NCEP reanalysis data, China raingauge precipitation data, CMAP precipitation data, and the MM5v3 mesoscale model, the zonal wind over the SCS and its adjacent areas is used to indicate variability of the SCS tropical monsoon intensity and the influences of the May–July SCS tropical monsoon anomalies on the YR monsoon and rainfall are investigated from observations and numerical simulations. The observational data analysis shows that on the interannual scale, the monsoon and rainfall over the MLRYR have an out-of-phase relationship with those over the SCS during June and July. When the tropical monsoon and rainfall are stronger (weaker), the northern boundary of the western Pacific subtropical ridge is southward, the southwest monsoon over the MLRYR is weaker (stronger), the tropospheric upward motion is weaker (stronger) over eastern China, and the local rainfall is generally less (more).

Numerical simulations show that for the years with a strong or weak southwest monsoon over eastern China, significant monsoon and rainfall variations appear over the MLRYR in response to the SCS tropical monsoon intensity change. This supports the results from the observational analysis. That is, when the westerly wind strengthens over the tropical monsoon region, the local rainfall increases, while the northern boundary of the western North Pacific subtropical ridge is more southward. Meanwhile, the southwest monsoon weakens over the land of eastern China, so does the local upward motion, which lead to the decreased rainfall over the East Asian subtropical monsoon region. This consistency between the observation and simulation not only demonstrates the rationality of the design of the numerical experiments in the present study but also indicates that the link between the SCS tropical and YR monsoon rainfalls may reflect an impact of the former on the latter. Moreover, on the interannual scale, the positive (negative) anomalies in the tropical westerly wind and rainfall maintain largely over the tropics during May and July and do not directly shift northward into the subtropics of eastern China, so the transport of water vapor toward southern China and the southwesterly wind and rainfall over the MLRYR are not increased (decreased). On the other hand, the tropical monsoon anomalies may result in the weakening and southward shift of the western Pacific subtropical high through adjustment of the atmospheric circulation, leading to the weakening of the YR monsoon. The impact of the tropical monsoon on the YR monsoon needs to be explained physically. Further thermodynamic and dynamic analyses should be performed in the future.

Moreover, it is not clear whether the observed out-of-phase relationship between the SCS tropical monsoon and the YR monsoon rainfall reflects an impact of the latter on the former. This also needs further studies with both dynamical analysis and numerical simulations.

REFERENCES

Chen Longxun and Xie An, 1988: Westward propagating low frequency oscillation and its teleconnection in the Eastern Hemisphere. *Acta Meteor. Sinica*, **2**(3), 300–312.

——, Zhu Qiangen, Luo Huibang, et al., 1991: *East Asian Monsoon*. China Meteorological Press, Beijing, 362 pp. (in Chinese)

——, Li Wei, Zhao Ping, et al., 2001: On the process of summer monsoon onset over East Asia. *Acta Meteor. Sinica*, **15**(4), 436–449.

Ding Yihui, 2004: Seasonal march of the East-Asian summer monsoon. *East Asian Monsoon*, Chang C. P., Ed., World Scientific, Singapore, 3–53.

——, Chen Longxun, and M. Murakami, 1994: *Asian Monsoon*. China Meteorological Press, Beijing, 263 pp. (in Chinese)

——, Li Chongyin, He Jinhai, et al., 2004: South China Sea Monsoon Experiment (SCSMEX) and the East Asian monsoon. *Acta Meteor. Sinica*, **62**(5), 561–586. (in Chinese)

—— and Liu Yanju, 2006: Simulation of the South China Sea summer monsoon onset. *Quart. J. Appl. Meteor.*, **17**(5), 526–537.

——, Wang Zunya, and Sun Ying, 2007: Interdecadal variation of the summer precipitation in East China and its association with decreasing Asian summer monsoon. Part I: Observed evidence. *Int. J. Climatol.*, **28**, 1139–1161.

Gemmill, W., B. Katz, and X. Li, 2007: Daily real-time global sea surface temperature high resolution analysis at NOAA/NCEP. NOAA/NWS/NCEP/MMAB Office Note No. 260, 39 pp.

He Jinhai and Yu Xinwen, 1986: A preliminary analysis of the periodic oscillation in water vapour transportation crossing different latitudes over the east of China. *J. Trop. Meteor.*, **2**(1), 9–15.

—— and Yang Song, 1992: Meridional propagation of East Asian low-frequency mode and midlatitude low-frequency waves. *Acta Meteor. Sinica*, **50**(2), 190–198. (in Chinese)

——, Qi Li, Wei Jin, et al., 2007: Re-investigations on the East Asian subtropical monsoon and tropical monsoon. *Chinese J. Atmos. Sci.*, **31**(6), 1257–1265.

Huang Ronghui and Li Weijing, 1988: Influence of the heat source anomaly over the tropical western Pacific on the subtropical high over East Asia and its physical mechanism. *Chinese J. Atmos. Sci.*, **14** (Special Issue), 95–107.

—— and Sun Fengying, 1994: Impact of the thermal state and convective activities over the western Pacific warm pool on summer climate anomalies in East Asia. *Chinese J. Atmos. Sci.*, **18**(2), 141–151.

——, Gu Lei, Xu Yuhong, et al., 2005: Characteristics of the interannual variations of onset and advance of the East Asian summer monsoon and their associations with thermal states of the tropical western Pacific. *Chinese J. Atmos. Sci.*, **29**(1), 20–36.

Kalnay, E., M. Kanamitsu, R. Kistler, et al., 1996: The NCEP/NCAR 40-year reanalysis project. *Bull. Amer. Meteor. Soc.*, **77**, 437–471.

Lau, K. H., A. Y. Wang, Y. H. Kuo, et al., 1998: The evolution of the East Asian summer monsoon in June 1994: Numerical simulations. *J. Meteor. Soc. Japan*, **76**, 749–764.

Lau, K. M., and S. Yang, 1997: Climatology and interannual variability of the Southeast Asian summer monsoon. *Adv. Atmos. Sci.*, **14**, 141–161.

Li Chongyin, Long Zhenxia, and Zhang Qingyun, 2001: Strong/weak summer monsoon activities over the South China Sea and the atmospheric intraseasonal oscillation. *Adv. Atmos. Sci.*, **18**, 1146–160.

Liu Changzheng, Wang Huijun, and Jiang Dabang, 2004: The configurable relationships between summer monsoon and precipitation over East Asia. *Chinese J. Atmos. Sci.*, **28**(5), 700–712.

Lu Riyu, 2004: Associations among the components of the East Asian summer monsoon system in the meridional direction. *J. Meteor. Soc. Japan*, **82**, 155–165.

Nitta, T., 1987: Convective activities in the tropical western Pacific and their impact on the Northern Hemisphere summer circulation. *J. Meteor. Soc. Japan*, **65**, 373–390.

Qi Li, He Jinhai, Zhang Zuqiang, et al., 2007: Seasonal cycle of the zonal land-sea thermal contrast and East Asian subtropical monsoon circulation. *Chinese Sci. Bull.*, **52**(24), 2895–2899.

Qian Weihong, 2009: *Global Climate System*. Peking University Press, Beijing, 232–283.

—— and Yang Song, 2000: Onset of the regional monsoon over Southeast Asia. *Meteor. Atmos. Phys.*, **75**, 29–38.

——, Zhu Jiang, Wang Yongguang, et al., 2009: Regional relationship between the Jiang-Huai Meiyu and the equatorial surface-subsurface temperature anomalies. *Chinese Sci. Bull.*, **54**(1), 79–84.

Tang Jianping, Su Bingkai, Zhao Ming, et al., 2004: Long term climate change numerical simulation in East Asia. *Acta Meteor. Sinica*, **62**(6), 752–763. (in Chinese)

Uppala, S. M., P. W. KÅllberg, A. J. Simmons, et al., 2005: The ERA-40 reanalysis. *Quart. J. Roy. Meteor. Soc.*, **131**, 2961–3012.

Wang Bin, Wu Renguang, and Fu Xiuhua, 2000: Pacific-East Asian teleconnection: How does ENSO affect East Asian climate? *J. Climate*, **13**, 1517–1536.

——, Lin Ho, Zhang Yongsheng, et al., 2004: Definition of South China Sea monsoon onset and commencement of the East Asian summer monsoon. *J. Climate*, **17**, 699–710.

——, Wu Zhiwei, Li Jianping, et al., 2008: How to measure the strength of the East Asian summer monsoon. *J. Climate*, **21**, 4449–4463.

Wang Huijun, 2002: The instability of the East Asian summer monsoon–ENSO relations. *Adv. Atmos. Sci.*, **19**, 1–11.

Webster, P. J., and S. Yang, 1992: Monsoon and ENSO: Selectively interactive systems. *Quart. J. Roy. Meteor. Soc.*, **125**, 611–633.

——, V. O. Magana, T. N. Palmer, et al., 1998: Monsoons: Processes, predictability, and the prospects for prediction. *J. Geophys. Res.*, **103**, 14451–14510.

Wen Zhiping, Huang Ronghui, He Haiyan, et al., 2006: The influences of anomalous atmospheric circulation over mid-high latitudes and the activities of 30–60 day low frequency convection over low latitudes on the onset of the South China Sea summer monsoon. *Chinese J. Atmos. Sci.*, **30**(5), 952–964.

Xie, P., and P. A. Arkin, 1997: Global precipitation: A 17-year monthly analysis based on gauge observations, satellite estimates, and numerical model outputs. *Bull. Amer. Meteor. Soc.*, **78**, 2539-2558.

Yao Cai and Qian Weihong, 2011: Interdecadal transitions and exceptional two years of June precipitation over South China. *J. Trop. Meteor.*, **26**(4), 463–469.

Zhang Qingyun and Tao Shiyan, 1998: Tropical and subtropical monsoon over East Asia and its influence on the rainfall over eastern China in summer. *J. Appl. Meteor. Sci.*, **9**(S1), 17–23. (in Chinese)

Zhang Renhe, 2001: Relations of water vapor transport from Indian monsoon with those over East Asia and the summer rainfall in China. *Adv. Atmos. Sci.*, **18**, 1005–1017.

Zhao Ping and Zhou Xiuji, 2001. Formation of low-level mesoscale south-west jet during seasonal rainfall. *Progress in Natural Sciences*, **11**(4), 272–279.

——, Zhang Renhe, Liu Jiping, et al., 2007: Onset of southewesterly wind over eastern China and associated atmospheric circulation and rainfall. *Climate Dyn.*, **28**, 797–811.

—— and Zhou Zijiang, 2009: An East Asian subtropical summer monsoon index and its relationship to summer rainfall in China. *Acta Meteor. Sinica*, **23**(1), 18–28.

——, Jiang Pinping, Zhou Xiuji, and Zhu Congwen, 2009a: Modeling impacts of East Asian ocean-land thermal contrast on spring southwesterly winds and rainfall in eastern China. *Chinese Sci. Bull.*, **54**, 4733–4741.

——, Zhou Xiuji, Chen Longxun, et al., 2009b: Characteristics of subtropical monsoon and rainfall over eastern China and western North Pacific. *Acta Meteor. Sinica*, **23**(6), 649–665.

——, Yang Song, and Yu Rucong, 2010: Long-term changes in rainfall over eastern China and large-scale atmospheric circulation associated with recent global warming. *J. Climate*, **23**, 1544–1562.

Zou Li and Ni Yunqi, 1997: Impact of ENSO on the variability of the summer monsoon over Asia and the summer rainfall in China. *J. Appl. Meteor. Sci.*, **13**(4), 306–314. (in Chinese)